The International Journal of Advanced Manufacturing Technology (2022) 121:1717–1730
https://doi.org/10.1007/s00170-022-09397-5

ORIGINAL ARTICLE

Experimental investigation on ultrasonic-assisted truing/dressing of diamond grinding wheel with cup-shaped GC wheel

Jiaping Qiao[1,2] · Hanqiang Wu[2] · Linhe Sun[2] · Ming Feng[3] · Jiang Zeng[2] · Yongbo Wu[2]

Received: 6 January 2022 / Accepted: 19 May 2022 / Published online: 2 June 2022

Abstract

In the mirror surface grinding of fine ceramics with diamond grinding wheels, the truing/dressing of wheels must be frequently performed to maintain the shape accuracy and abrasive cutting-edge sharpness of the diamond grinding wheels to ensure a high processing efficiency and precision. For this purpose, a novel method is proposed for truing/dressing diamond grinding wheels in which a cup-shaped GC (Green silicon carbide) wheel is used as the truing/dressing tool and an ultrasonic vibration is applied axially to the diamond grinding wheel during truing/dressing. A truing/dressing device was designed and fabricated, and a series of experiments were conducted to systematically investigate the truing/dressing characteristics of metal–resin-bonded diamond grinding wheels. The following conclusions have been obtained. The truing/dressing force F_x is decreased with an increase of the ultrasonic amplitude. After truing/dressing, the performance of the grinding wheel has been significantly improved, including the improvement of shape accuracy and the increase in the number of effective abrasive particles per unit area with the assistance of ultrasonic vibrations during truing/dressing. Moreover, during truing/dressing, the introduction of the ultrasonic vibration reduced the abrasive grain cutting-edge apex angle, meaning that the sharpness of the grain cutting edge was improved by the ultrasonic vibrations. The truing/dressing ratio increased with an increase in the ultrasonic amplitude, leading to an extension of the servicing life of the cup-shaped GC wheel. Finally, a comparison of the performance of the grinding wheels trued/dressed with and without ultrasonic vibrations during the grinding of zirconia ceramics revealed that the grinding wheel trued/dressed with ultrasonic vibrations yielded an enhanced machined surface quality and lower grinding forces.

Keywords Ultrasonic-assisted truing/dressing · Cup-shaped GC wheel · Metal–resin-bonded · Diamond grinding wheel

✉ Yongbo Wu
wuyb@sustech.edu.cn

Jiaping Qiao
11749328@mail.sustech.edu.cn

Hanqiang Wu
12031212@mail.sustech.edu.cn

Linhe Sun
12032419@mail.sustech.edu.cn

Ming Feng
fming@wzu.edu.cn

Jiang Zeng
zengj@sustech.edu.cn

[1] Harbin Institute of Technology, Harbin 150000, China

[2] Southern University of Science and Technology, Shenzhen 518055, China

[3] College of Mechanical and Electrical Engineering, Wenzhou University, Wenzhou 325035, China

1 Introduction

With the popularization of advanced engineering materials, such as fine ceramics, optical glass, semiconductors, and other difficult-to-machine materials in the engineering field, the diamond grinding technique has played an increasingly important role in the precise and efficient machining of these advanced hard/brittle materials, because the required machining efficiency, machining accuracy, and grinding wheel working life can be more easily achieved with diamond grinding wheels than with other processing methods [1, 2]. As a typical application of diamond grinding, the present authors conducted an experimental study on tangential ultrasonic-assisted grinding for obtaining mirror surfaces of zirconia ceramics using metal–resin-bonded diamond wheels and confirmed the advantages of the diamond grinding wheel [3]. However, it was found that to ensure processing efficiency and precision, the diamond wheel must

be reconditioned frequently to maintain the shape accuracy and abrasive cutting-edge sharpness. The reconditioning of a grinding wheel includes truing and dressing. Owing to the manufacturing and installation errors of the grinding wheel and the wheel wear in use, the wheel shape accuracy often does not meet the requirements. In particular, the acquisition of a mirror surface is directly affected by the wheel shape accuracy. Therefore, the diamond grinding wheel must be quickly and effectively trued whenever necessary. In addition, because the sharpness of the grinding wheel is mainly determined by the protrusion height and distribution of abrasive grains, the grinding wheel needs to be frequently dressed to obtain the required protrusion height and distribution density of grains and maintain the required grinding performance.

Several studies have indicated that the wheel truing/dressing technology not only affects the processing efficiency and quality but also affects the working life of the grinding wheel [4, 5]. The important indices to evaluate the pros and cons of wheel truing/dressing methods include the truing/dressing efficiency, the number of effective abrasive grains, and the shape accuracy of the grinding wheel. At present, the commonly used truing/dressing methods of diamond grinding wheels are the cup-shaped green silicon carbide (GC) wheel dressing method [6–8], electrical discharge dressing method [9–11], electrolytic in-process dressing (ELID) method [12], and laser dressing method [13]. These methods have improved the grinding wheel performance to a certain extent. However, with the increasing requirements of machining accuracy, efficiency, and costs of practical applications, these methods also have their respective limitations. In the cup-shaped GC wheel dressing method, the truing/dressing operation is generally performed by facing the end face of the GC wheel to the diamond grinding wheel working surface. During truing/dressing, the GC abrasive grains are broken or fall off to form free abrasive grains, which remove the bond materials of the grinding wheel. Consequently, a higher truing/dressing efficiency and better grinding wheel surface morphology can be obtained, but the GC wheel wears quickly. Furthermore, the straightness of the grinding wheel after truing/dressing is poor, and in particular, the bond tail phenomenon occurs frequently [14, 15]. The electrical discharge dressing method can effectively remove the bond materials of the grinding wheel by discharge, but it is only suitable for conductive grinding wheels, and the dressing efficiency is low. In addition, a large amount of heat generated during discharge will lead to a certain degree of graphitization of the diamond grains, and a specialized power supply with a high-frequency pulse should be also equipped [16, 17]. For a conductive grinding wheel, the ELID method is suitable for its sharpening quality, especially for fine-grained conductive grinding wheels. However, the truing ability is poor, and complex dressing devices and environmentally unfriendly electrolytes are needed [18, 19]. The laser dressing method does not require a processing medium and materials such as coolants, and it can yield a better shape accuracy of the grinding wheel. However, this method will inevitably damage the abrasive grains and reduce the grinding performance while removing the bond materials at high temperatures. Moreover, maintenance of laser dressers is expensive and difficult, and it is greatly affected by the production site environment [13].

In summary, for the truing/dressing of metal–resin-bonded diamond grinding wheels, it is difficult to apply either the electrical discharge dressing method or the ELID method due to the poor conductivity, while the laser dressing method is still immature and the equipment is relatively expensive. In contrast, the cup-shaped GC wheel dressing method has the advantages of a simple operation and easy realization of online truing/dressing. In the preliminary study of tangential ultrasonic-assisted mirror grinding of zirconia ceramics using metal–resin-bonded diamond grinding wheels, the cup-shaped GC wheel dressing method was used for truing/dressing of the grinding wheel, and a mirror surface was successfully achieved on the zirconia ceramic workpiece. It was proven that the cup-shaped GC wheel dressing method is very effective in the precision truing/dressing of metal–resin-bonded diamond grinding wheels [3]. However, at the same time, it was also found that when this method was used, the improvement of the truing/dressing accuracy was slow, and the required abrasive grain distribution and protrusion height were relatively time consuming, indicating that the truing/dressing efficiency needs to be further improved. In previous research, the present authors proposed an ultrasonic-assisted cup-shaped GC wheel dressing method. That is, when the cup-shaped GC wheel was used to true/dress the grinding wheel, an axial ultrasonic vibration was applied to the grinding wheel. The performance of this method on the truing/dressing of a vitrified cubic boron nitride (cBN) grinding wheel was also studied, and it was preliminarily verified that the ultrasonic vibrations could effectively improve the truing/dressing efficiency [20].

Based on the previous research results, the ultrasonic-assisted cup-shaped GC wheel dressing method was applied for the truing/dressing of a metal–resin-bonded diamond grinding wheel in this study. First, the research background and purpose are introduced, and then the truing/dressing principle is described in detail, and the corresponding experimental apparatus is outlined. The influence of ultrasonic vibrations on the truing/dressing characteristics (truing/dressing force, grinding wheel shape accuracy, and effective number of abrasive grains) was systematically studied using an experimental apparatus. The mechanism of ultrasonic-assisted truing/dressing of the grinding wheel was analyzed, and the truing/dressing conditions were optimized. Finally,

the mirror surface grinding of zirconia ceramics was conducted with a diamond grinding wheel trued/dressed by the ultrasonic-assisted cup-shaped GC wheel dressing method to confirm the effectiveness of the proposed novel truing/dressing method.

2 Truing/dressing principle, experimental apparatus, and procedure

2.1 Truing/dressing principle

Figure 1 shows the schematic diagram of the ultrasonic-assisted truing/dressing principle of the grinding wheel with a cup-shaped GC wheel. As shown in Fig. 1a, the grinding wheel and the GC wheel rotate at speeds n_g and n_d, respectively, and the grinding wheel is subjected to an ultrasonic vibration of frequency f and amplitude $A_{p\text{-}p}$ in its axial direction. In the truing/dressing process, as shown in Fig. 1b, the grinding wheel reciprocates left and right in the range from O_1 to O_2 along the radial direction of the GC wheel at a speed of V_f, and the distance between O_1 and O_2 is S. The value of S is slightly larger than the wall thickness of the GC wheel, that is, $S \geq R_{outer} - R_{inner}$ (R_{inner} and R_{outer} are the inner and outer radii of the cup-shaped GC wheel, respectively), so that the entire cup-shaped GC wheel participates in the truing/dressing process. Each time from O_1 to O_2 or from O_2 back to O_1, a truing/dressing depth of cut δ is applied to the grinding wheel along the axis of the GC wheel. Then, the reciprocating motion is repeated until the radial runout of the grinding wheel is reduced to below the target value. During truing/dressing, a small amount of grinding coolant is supplied through the nozzle.

The material removal mechanism in the ultrasonic-assisted truing/dressing of the diamond grinding wheel with a cup-shaped GC wheel is shown in Fig. 1c and d. During truing/dressing, as shown in Fig. 1c, the GC abrasive grains of the cup-shaped wheel collide with the bond materials and occasionally with the diamond grains of the grinding wheel. Owing to the cutting action of the GC abrasive grains on the bond materials, the protrusion height of the diamond grains increases with the removal of the surrounding bond materials, and some diamond grains will fall off, achieving the purpose of truing/dressing. Conversely, because the hardness of the diamond grains is much higher than that of the GC grains, some of the GC grains will be broken and will fall off from the cup-shaped wheel when colliding with diamond grains. Subsequently, the broken and fallen GC grains will grind and will remove the bond materials in a small amount of grinding coolant, which further promotes the truing/dressing of the grinding wheel.

If an axial ultrasonic vibration (frequency f, amplitude $A_{p\text{-}p}$) is applied to the grinding wheel at this time, as shown in Fig. 1d, the relative movement trajectory of the GC grains on the GC wheel or those that have been broken and fallen off onto the peripheral surface of the diamond

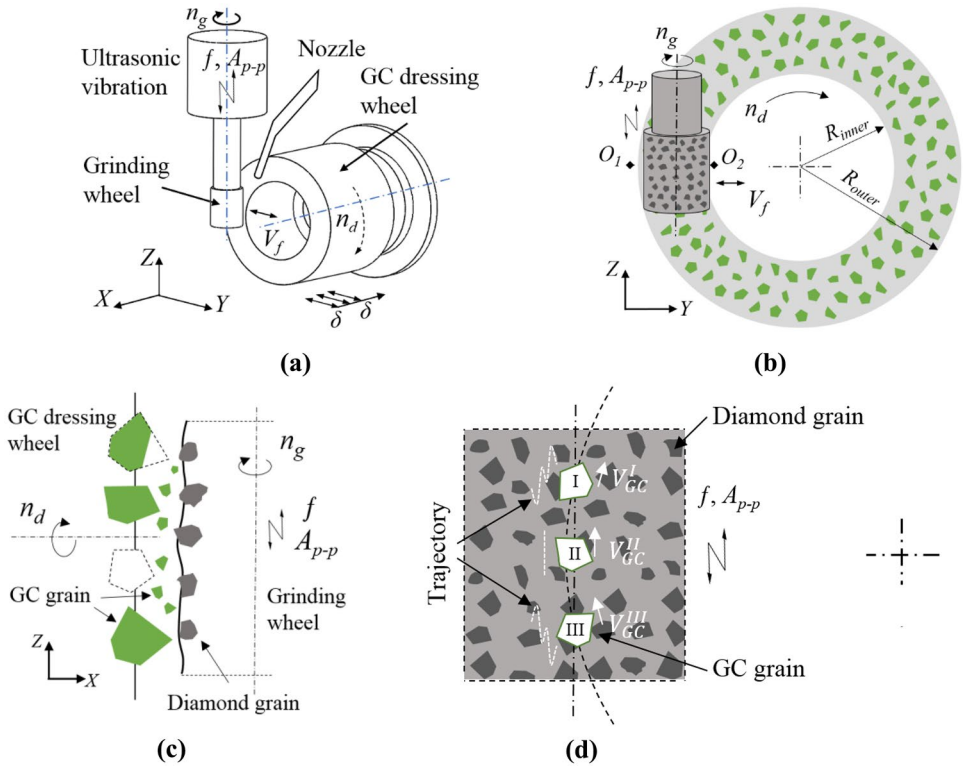

Fig. 1 Schematic diagram of ultrasonic-assisted truing/dressing principle with a cup-shaped GC wheel. **a** Three-dimensional illustration of ultrasonic-assisted truing/dressing of the grinding wheel, **b** *X*-direction view, **c** *Y*-direction view, **d** trajectory of GC grains

wheel will result in an irregular, fluctuating curve along the velocity V_{GC} direction of the GC grains. However, the GC grains whose velocities are parallel to the axis of the grinding wheel, such as GC grain II in Fig. 1d, whose velocity is V_{GC}^{II}, only vibrate back and forth along the axis of the grinding wheel. The movement directions and velocities of the GC grains may change at any time during truing/dressing, and the velocities of GC grains I and III in Fig. 1d are V_{GC}^{I} and V_{GC}^{III}, respectively. The trajectories of different GC grains intersect with each other, thereby further improving the removal rate of the bond materials and yielding a higher truing/dressing efficiency. In addition, ultrasonic vibrations can generate cavitation, which increases the cutting and erosion effect of the abrasive grains on the bond materials and further effectively removes the bond tails [21].

2.2 Experimental apparatus

Figure 2 shows a photograph of the experimental apparatus used to realize the above-mentioned truing/dressing principle. The apparatus was constructed by installing a dressing device on the worktable of a CNC (computer numerical control) machining center (GX1000 PLUS by Hardinge Inc.) equipped with an ultrasonic spindle (UB40-C5-BT40 by Takesho Co., Ltd.). Under the dressing device, a piezoelectric dynamometer (Kistler 9119A) was installed on the worktable to measure the truing/dressing force, and a laser displacement sensor (Keyence LK-G35) was installed near the dressing device on the worktable to measure the radial runout and axial straightness of the grinding wheel. During truing/dressing, the dressing device could perform reciprocating motions along *Y*-axis together with the worktable, and the truing/dressing depth of cut was determined by the movement of the worktable along *X*-axis. The coolant was supplied to the truing/dressing area through the nozzle. The metal–resin-bonded diamond grinding wheel (SD4000125MSH, 8 mm in diameter) was mounted on the end of the ultrasonic spindle. The ultrasonic frequency of the grinding wheel was $f = 27$ kHz, and its ultrasonic vibration amplitude could be adjusted in the range of 0–5 μm.

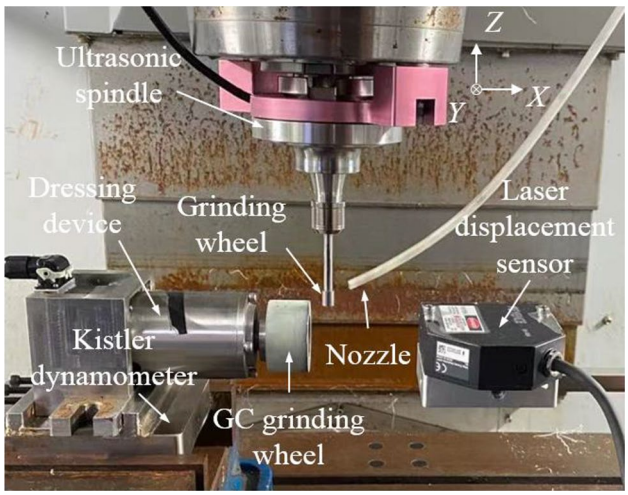

Fig. 2 Photograph of the experimental apparatus constructed for ultrasonic-assisted truing/dressing of the diamond grinding wheel with a cup-shaped GC wheel

To evaluate the truing/dressing effect, in addition to directly measuring the radial runout and axial straightness of the grinding wheel as well as the distribution of effective diamond grains on the grinding wheel working surface after truing/dressing, grinding tests involving zirconia ceramic workpieces were also conducted with the trued/dressed grinding wheel to characterize the grinding force and the work surface roughness to indirectly evaluate the truing/dressing effect. Figure 3 shows a schematic diagram of the experimental process from truing/dressing at position ① to grinding at position ②. The mechanism for holding the workpiece consisted of the same dynamometer that was used in the truing/dressing and a workpiece holder, which were installed at a different position from that of the dressing device on the worktable of the CNC machining center used in the truing/dressing. A metal–resin-bonded diamond grinding wheel was mounted on the end face of the ultrasonic spindle. In the experiment, the diamond wheel was first trued/dressed at position ① and then moved to position ② to perform the grinding operation.

2.3 Experimental method and conditions

The previous work on the tangential ultrasonic-assisted grinding of zirconia ceramics by the present authors showed that when a metal–resin-bonded diamond wheel was trued/dressed at $n_d = 500$ rpm, $n_g = 1500$ rpm, and $V_f = 40$ mm/min without ultrasonic vibrations and used in grinding operations, a mirrorlike work surface was successfully obtained [3]. Therefore, because the purpose of this study was to clarify the influence of the ultrasonic amplitude on the truing/dressing of metal–resin-bonded diamond grinding wheel and the dressing device utilized in the previous work was

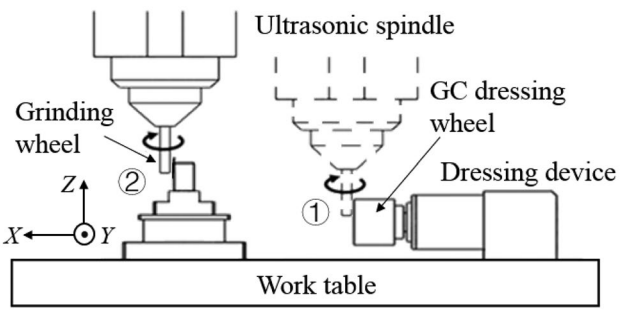

Fig. 3 Layout for grinding experiment

Table 1 Truing/dressing conditions

Ultrasonic vibration	Frequency f	27 kHz
	Amplitude $A_{p\text{-}p}$	0–5 μm
Grinding wheel	SD4000125MSH (8 mm in diameter, 10 mm in length)	
	Rotational speed n_g	1500 rpm
	Truing/dressing depth of cut δ	3 μm/pass
	Reciprocation speed V_f	40 mm/min
Cup-shaped GC wheel	GC1000V (ϕ50 mm in outer diameter, ϕ30 mm in inner diameter, 20 mm in thickness, resulting in $S = 10$ mm)	
	Rotational speed n_d: 500 rpm	
Coolant	Solution type, 10.1% dilution	

also used in the current work, the values of n_d, n_g, and V_f were fixed at $n_d = 500$ rpm, $n_g = 1500$ rpm, and $V_f = 40$ mm/min, respectively. Only the ultrasonic amplitude was varied in the range of $A_{p\text{-}p} = 0$–5 μm, where $A_{p\text{-}p} = 0$ μm was for the truing/dressing without ultrasonic vibrations. Each group of truing/dressing experiments was repeated six times, and the average values of six data (e.g., shape accuracy and abrasive grain distribution) were taken as the experimental results of the group. At the same time, grinding wheels produced in the same batch were used to avoid large differences between their initial states. Table 1 shows the experimental parameters.

As one of the evaluation indices of the truing/dressing effect, the radial runout of the diamond wheel was measured by the method shown in Fig. 4. As shown in Fig. 4a, the laser displacement sensor was located at a vertical distance L from the upper end face of the grinding wheel, and the distance between the grinding wheel and the laser displacement sensor in the horizontal direction was fixed at $\acute{L}$ ($5\text{ mm} < \acute{L} < 10$ mm) based on the technical specifications of

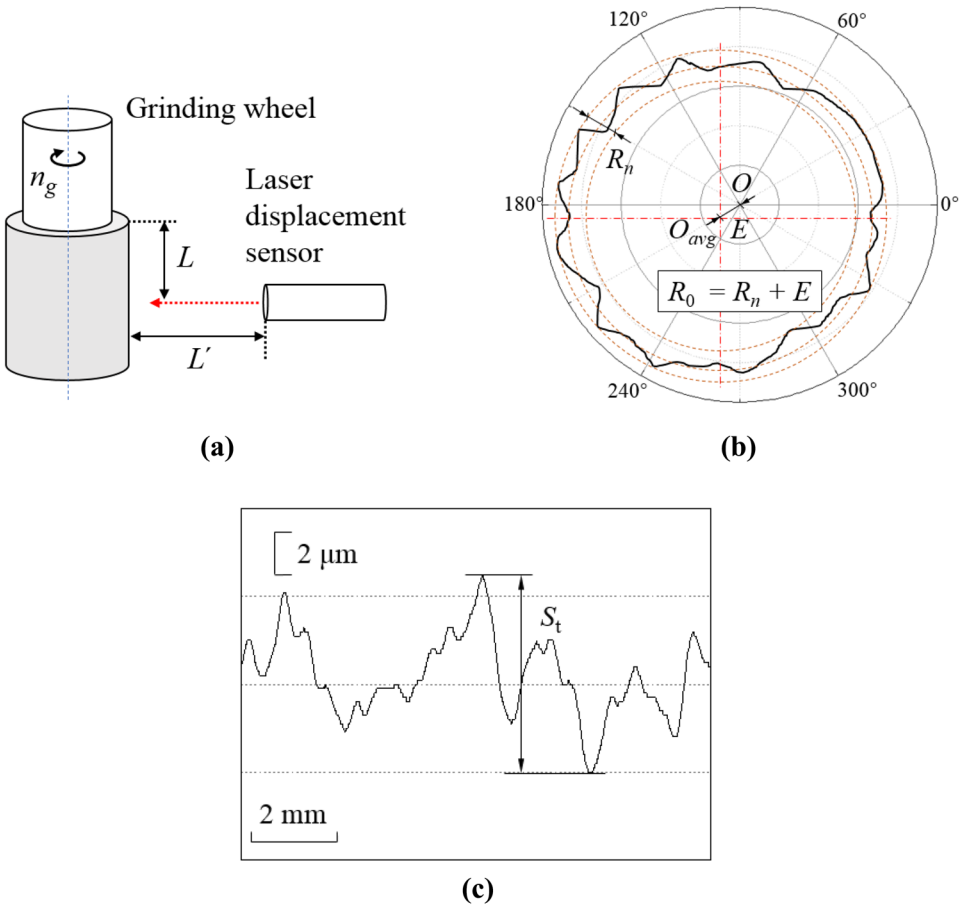

Fig. 4 Diagram of characterization method for shape error measurement. **a** Measurement schematic, **b** method for calculating radial runout, **c** method for calculating straightness error

the laser displacement sensor. The grinding wheel was then rotated at a lower speed. At this time, the distance between the laser displacement sensor and the outer circumference of the grinding wheel varied with the wheel rotation if there was radial runout of the grinding wheel. As a result, the cross-sectional profile of the grinding wheel was obtained, as shown in Fig. 4b, and eventually, the wheel radial runout R_0 was obtained, which was composed of the eccentricity E (the distance between the wheel average circle center O_{avg} and the wheel rotation center O) and the wheel roundness error R_n, i.e., $R_0 = E + R_n$. This measurement was repeated at three different axial positions of the grinding wheel with different values of L, and the average of the obtained three data was taken as the result of this group of measurements. When measuring the straightness of the grinding wheel, the vertical and horizontal positions of the laser displacement sensor were fixed, and the non-rotating grinding wheel was moved vertically along its axis at a certain speed. Consequently, the wheel straightness error S_t could be obtained from the output of the laser displacement sensor, as shown in Fig. 4c. This measurement was also repeated three times at three different positions at intervals of 120° along the wheel circumference, and the average value of the obtained three data was taken as the wheel straightness error at the current measurement.

As another evaluation index of the grinding wheel truing/dressing effect, the distribution of diamond grains on the wheel working surface and the shape of the grain cutting edge were quantitatively obtained by scanning electron microscopy (SEM). In addition, the wear state of the cup-shaped GC wheel is also an important indicator to evaluate the truing/dressing effect. In this study, the truing/dressing ratio, which is the ratio of the volume reduction of the diamond wheel to the wear volume of the cup-shaped GC wheel in a given truing/dressing time, is introduced to quantitatively characterize the wear of the GC wheel. The volume reduction of the diamond wheel and the wear amount of the GC wheel can be obtained by measuring the radii of the diamond wheel and the GC wheel with the laser displacement sensor before and after truing/dressing. The initial radius of the diamond wheel and its reduction after truing/dressing are denoted as r_0 and Δr, respectively, and the volume reduction of the grinding wheel ΔV_{gw} can be calculated as follows:

$$\Delta V_{gw} = \pi r_0^2 l - \pi (r_0 - \Delta r)^2 l = 2\pi r_0 \Delta r l + \pi \Delta r^2 l, \tag{1}$$

where l is the length of diamond wheel. Since Δr is much smaller than r_0, the term $\pi \Delta r^2 l$ of Eq. (1) can be ignored, and Eq. (1) can be simplified as follows:

$$\Delta V_{gw} = 2\pi r_0 \Delta r l. \tag{2}$$

Similarly, the initial thickness of the GC wheel and the GC wheel thickness reduction after truing/dressing are denoted as t_0 and Δt, respectively. The volume reduction of the GC wheel ΔV_{dw} can be calculated as follows:

$$\Delta V_{dw} = \pi (R_{outer}^2 - R_{inner}^2) \Delta t, \tag{3}$$

where R_{outer} and R_{inner} are the outer and inner diameters of the GC wheel, respectively. Consequently, the truing/dressing ratio ξ can be calculated as follows:

$$\xi = \Delta V_{gw} / \Delta V_{dw} = 2 r_0 \Delta r l / (R_{outer}^2 - R_{inner}^2) \Delta t. \tag{4}$$

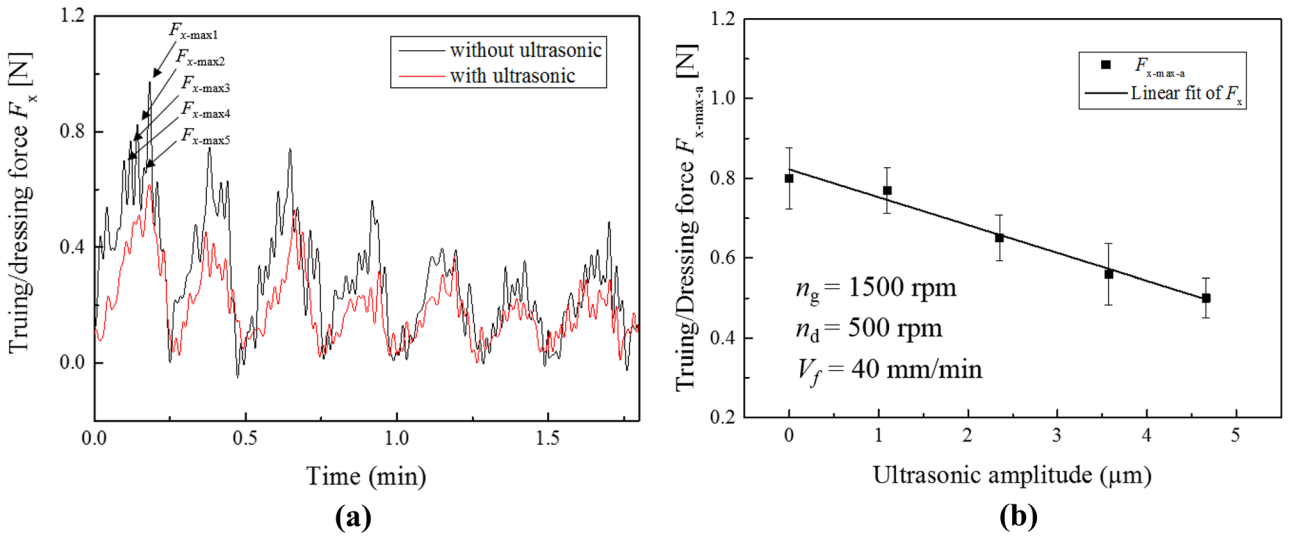

Fig. 5 Truing/dressing force F_x experimentally obtained. **a** Variations of truing/dressing force F_x with time at $A_{p\text{-}p} = 0$ and 4.7 μm, **b** Truing/dressing force F_x at different ultrasonic amplitudes in the first period

In addition, as the truing/dressing force is an important parameter for analyzing and discussing the influence of the ultrasonic vibrations on the truing/dressing characteristics, it was measured with the piezoelectric dynamometer located under the dressing device. In grinding tests with the trued/dressed grinding wheel, the work surface quality was characterized in terms of the surface morphology and surface roughness using a white light interferometer (Taylor Hobson CCI HD).

3 Results and discussion

3.1 Truing/dressing force

Figure 5a shows the variations of the normal truing/dressing force F_x in the X-direction during truing/dressing with or without ultrasonic vibrations. Regardless of whether there were ultrasonic vibrations, F_x exhibited periodic variations during truing/dressing, with a period of 15 s, which was

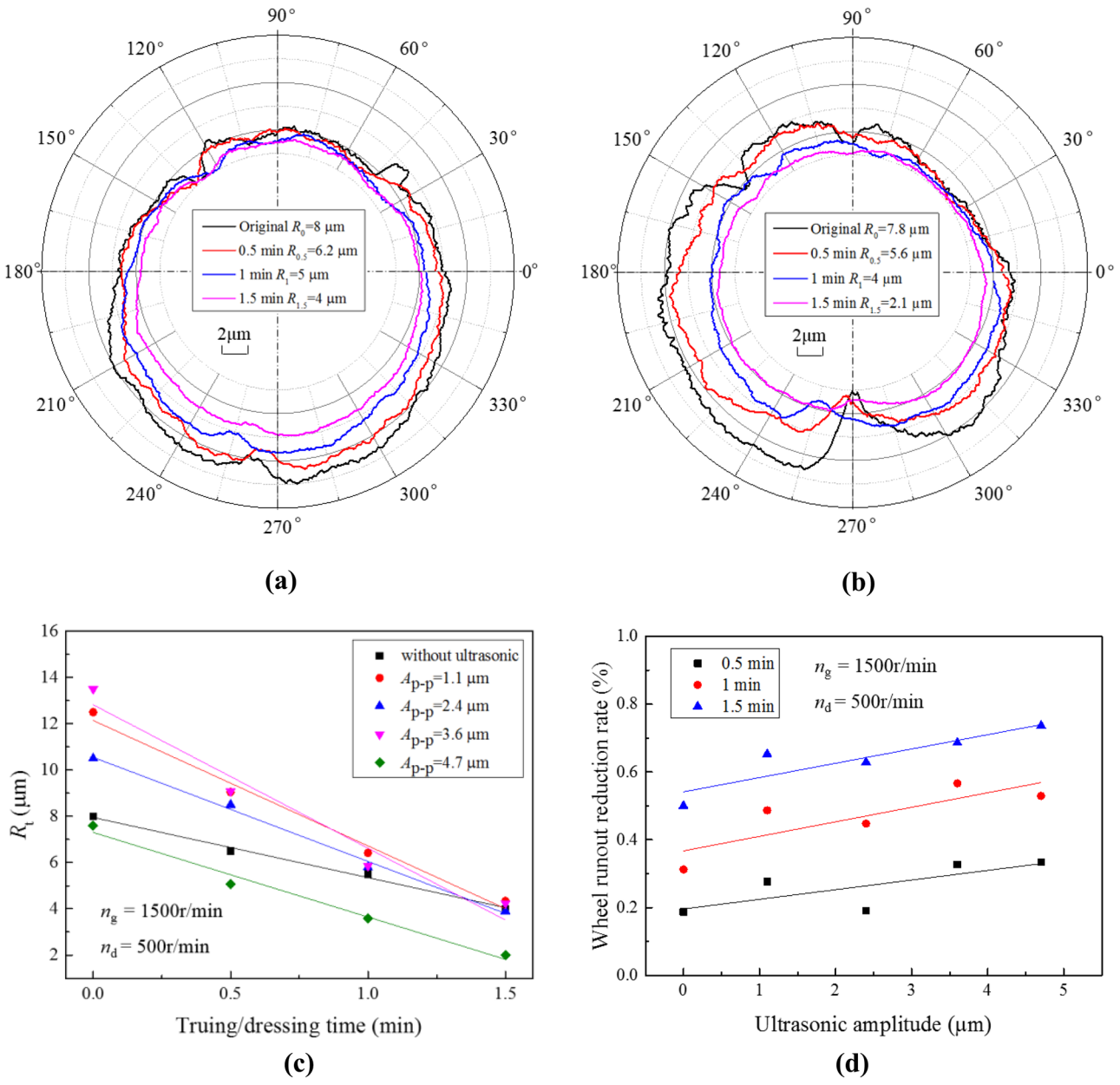

Fig. 6 Experimental results for wheel runout. **a** Typical runout of a wheel after truing/dressing for different times without ultrasonic vibrations, **b** typical runout of a wheel after truing/dressing for different times with ultrasonic vibrations at $A_{p\text{-}p}$=4.7 μm, **c** variations of wheel runout with truing/ dressing time for different $A_{p\text{-}p}$ values, **d** variations of wheel runout reduction rate with ultrasonic amplitude at different times

exactly the time required for the diamond grinding wheel to cut out the cup-shaped GC wheel from position O_1/O_2 to position O_2/O_1. However, F_x fluctuated violently in each period, resulting from the variation of the actual value of δ (Fig. 1a) with the grinding wheel rotation caused by the radial runout of the grinding wheel. Meanwhile, the peak value of F_x decreased gradually. This may have been because the wheel radial runout error decreased during truing/dressing, resulting in a gradual decrease in the variation magnitude of the actual δ. Furthermore, the peak value of F_x in the presence of ultrasonic vibrations was smaller than that without ultrasonic vibrations, indicating that the assistance of ultrasonic vibrations reduced the truing/dressing force.

The frequency of the change in depth of cut should be equal to the revolution speed of the grinding wheel, that is, there will be at least one F_x peak in each grinding wheel revolution. To quantitatively evaluate the influence of the ultrasonic vibrations on the truing/dressing force, the relationship between the average peak value $F_{x\text{-max-a}}$ ($= \frac{1}{5}\sum_{i=1}^{5} F_{x-\max i}$, where $F_{x\text{-max }i}$ ($i = 1, 2, \ldots, 5$) denotes the i_{st} highest peak value of truing/dressing force in the first truing/dressing period, as shown in Fig. 5a) and the ultrasonic amplitude was obtained, as shown in Fig. 5b. Evidently, the value of $F_{x\text{-}max\text{-}a}$ decreased monotonically with the increase in the amplitude in the range of 0–4.7 μm, implying that a larger amplitude will result in a higher shape accuracy of the grinding wheel.

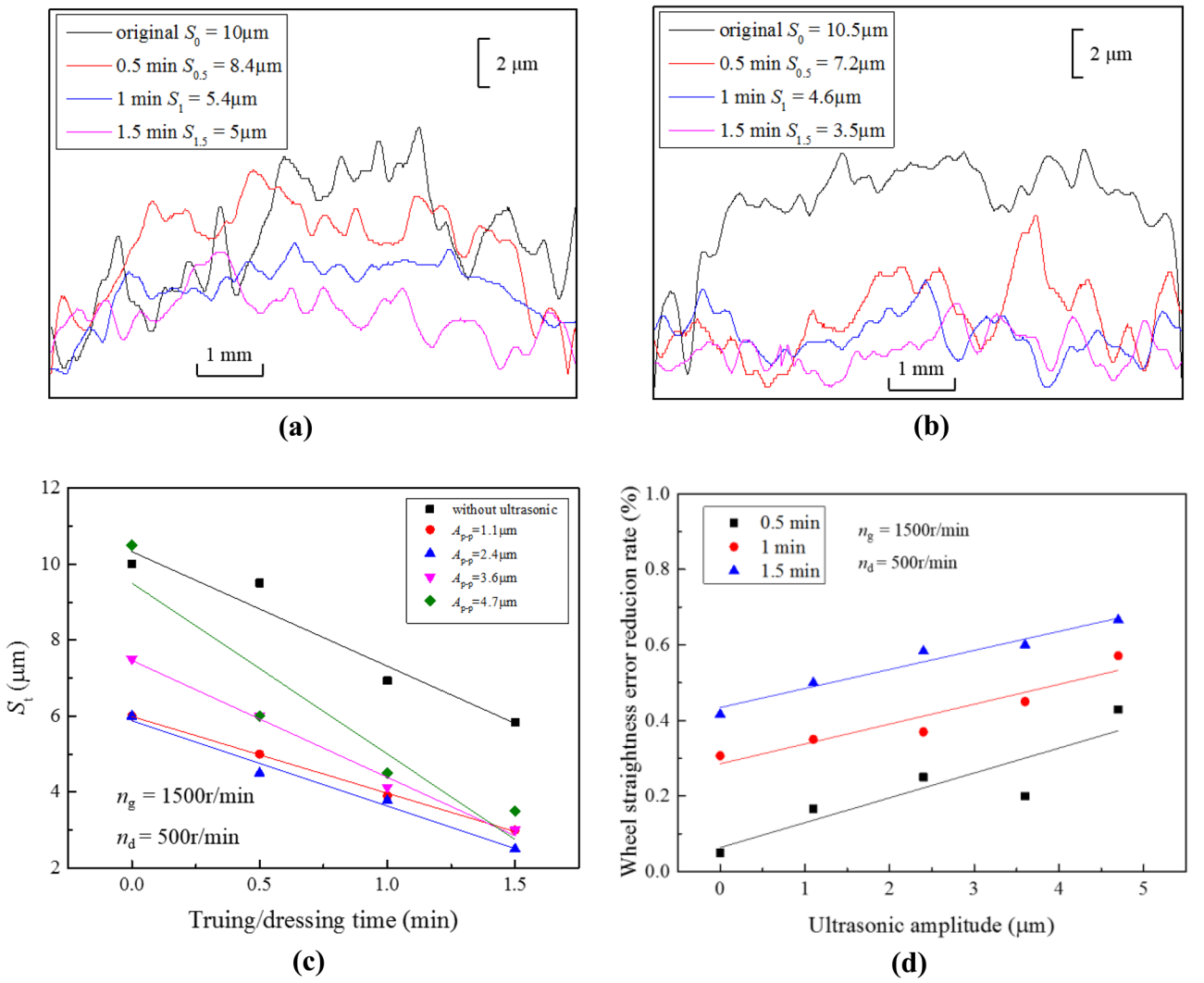

Fig. 7 Experimental results for wheel straightness. **a** Typical straightness of grinding wheel after truing/dressing for different times without ultrasonic vibrations, **b** typical straightness of grinding wheel after truing/dressing for different times with ultrasonic vibrations at $A_{p\text{-}p}$ = 4.7 μm, **c** variations of wheel straightness with truing/ dressing time for different $A_{p\text{-}p}$ values, **d** wheel straightness error reduction rates at different ultrasonic amplitudes for different truing/dressing times

3.2 Shape accuracy

The shape accuracy of the grinding wheel trued/dressed with or without ultrasonic vibrations was measured, and the typical radial runout and axial straightness obtained for different truing/dressing times are shown in Figs. 6 and 7, respectively. Figure 6a and b shows the cross-sectional profiles and radial runout of the grinding wheel at the middle position along its axial direction before and after truing/dressing for different times with ($A_{p\text{-}p}=4.7$ μm) and without ($A_{p\text{-}p}=0$ μm) ultrasonic vibrations, respectively. The wheel radial runouts showed downward trends with the truing/dressing time both with and without ultrasonic vibrations, but the reduction rate of the radial runout with ultrasonic vibrations was higher than that without. Specifically, in the absence of ultrasonic vibrations, the wheel radial runout decreased from 8 to 4 μm, i.e., by 50%, after 1.5 min, whereas in the presence of ultrasonic vibrations with the same truing/dressing time of 1.5 min, the wheel radial runout decreased from 7.8 to 2.1 μm, i.e., by 73%, demonstrating that the ultrasonic vibrations had a positive effect on the improvement of the shape accuracy. Furthermore, the wheel radial runouts at different truing/dressing times with different ultrasonic amplitudes are shown in Fig. 6c, indicating that the reduction rate of the wheel radial runout in the truing/dressing varied with the ultrasonic amplitude. The wheel runout reduction rates under different amplitudes for different truing/dressing times were calculated by a formula of $(R_0-R_t)/R_0$ and shown in Fig. 6d. The runout reduction rate increased with the increase in the amplitude, that is, a larger amplitude could bring about a higher truing/dressing efficiency. When the amplitude was $A_{p\text{-}p}=4.7$ μm, the radial runout after 1.5 min of truing/dressing was reduced by 73%, while that after 1.5 min of truing/dressing without ultrasonic vibrations was only reduced by 50%, i.e., the difference between the two was 23%.

Shifting the attention to the axial straightness of the grinding wheels, Fig. 7a and b shows the typical axial straightness before and after truing/dressing for different times measured at 0° in the wheel circumferential direction (Fig. 4b) with and without ultrasonic vibrations, respectively, where S_0 is the original straightness error before truing/dressing. Evidently, either with or without ultrasonic vibrations, the wheel straightness errors showed downward trends during truing/dressing. Specifically, it is worth noting that the straightness error decreased from 10 to 5 μm, i.e., by 50%, after 1.5 min of truing/dressing without ultrasonic vibrations, whereas the straightness error after truing/dressing with ultrasonic vibrations for the same time reached decreased from 10.5 to 3.5 μm, i.e., by 67%. Moreover, Fig. 7c shows that the wheel straightness error decreased with the truing/dressing time at different rates under different values of $A_{p\text{-}p}$. Similar to the case of wheel radial runout mentioned above, the reduction rates of the wheel straightness error under different ultrasonic amplitudes were obtained for different times by the formula $(S_0-S_t)/S_0$, as shown in Fig. 7d. Evidently, the reduction rate increased with the increase in $A_{p\text{-}p}$, resulting from the increase in the contact area between the grinding wheel and the cup-shaped GC wheel.

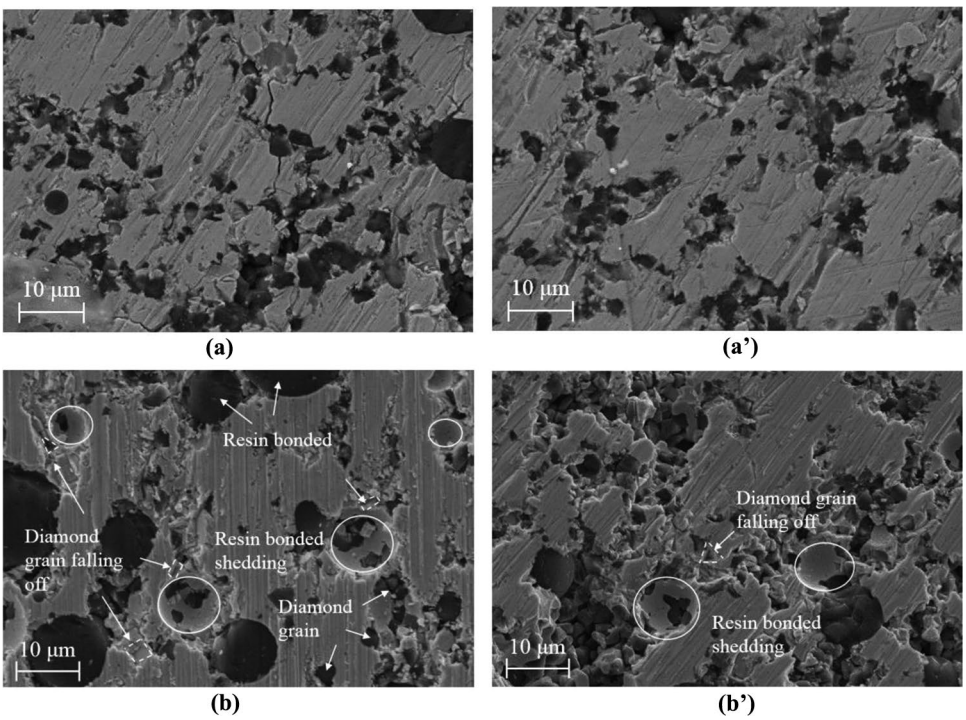

Fig. 8 Working surface morphology of grinding wheel before and after truing/dressing with and without ultrasonic vibrations. **a** Before truing/dressing without ultrasonic vibrations, a' before truing/dressing with ultrasonic vibrations, **b** after 1.5 min truing/dressing without ultrasonic vibrations, b' after 1.5 min truing/dressing with ultrasonic vibrations at $A_{p\text{-}p}=4.7$ μm

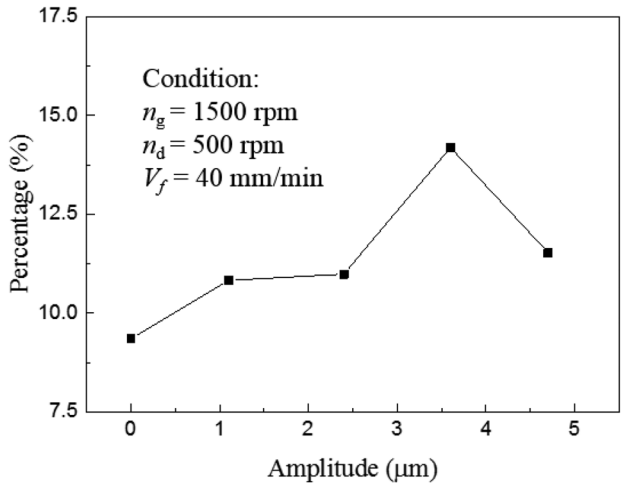

Fig. 9 Effect of ultrasonic amplitude on the proportion of effective abrasive grains

The above-mentioned results showed that the truing/dressing efficiency can be improved by the assistance of ultrasonic vibrations, and a higher ultrasonic amplitude will lead to a higher wheel shape accuracy. It is speculated that the truing/dressing force F_x decreases with the increase in the ultrasonic amplitude, resulting in the promotion of the stiffness and stability and an inhibition of the elastic deformation and low-frequency chatter of the truing/dressing system, eventually improving the wheel shape accuracy.

3.3 Distribution of effective abrasive grains

As previously mentioned in Sect. 2.3, the distribution of the effective abrasive grains on the working surface of the grinding wheel after truing/dressing is also an important index to evaluate the truing/dressing effect. In order to facilitate the analysis, the effective abrasive grains refer to the diamond abrasive grains that protrude from the bonder to a certain height, and may not actually participate in the grinding process. Among the effective abrasive grains, a certain proportion of diamond abrasive grains will participate in the grinding process and become active grains, which refers to the diamond abrasive grains that participate in the grinding process. However, these have a certain randomness and are affected by many factors. The active grains count depends on the depth of cut, the type of wheel, and the nature of the workpiece material [22, 23]. In general, abrasive grains with protrusion heights of more than one third of their diameters over the surrounding bond material are judged to be effective. As 4000# grinding wheels with grains of 3.7 μm in mean diameter were used in this work, the protrusion height should be more than 1.25 μm. However, in consideration of the presence of a large number of abrasive grains with diameters less than the mean grain diameter, the value of 1 μm for the effective abrasive grains was chosen to obtain statistics of the measurement process. As shown in Fig. 8, almost no difference in the distribution of the effective abrasive grains (Fig. 8a and a') was evident on the working surfaces of the two grinding wheels

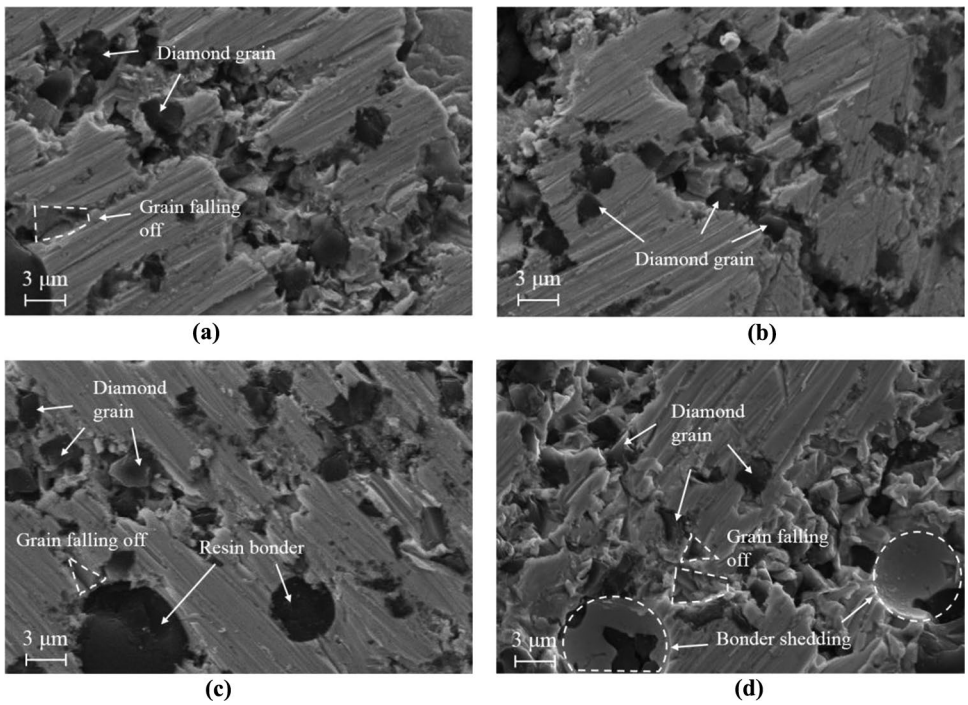

Fig. 10 Falloff of diamond grains and bond material on the surface of the grinding wheel with different ultrasonic amplitudes. **a** $A_{p\text{-}p}$ = 1.1 μm, **b** $A_{p\text{-}p}$ = 2.4 μm, **c** $A_{p\text{-}p}$ = 3.6 μm, **d** $A_{p\text{-}p}$ = 4.7 μm

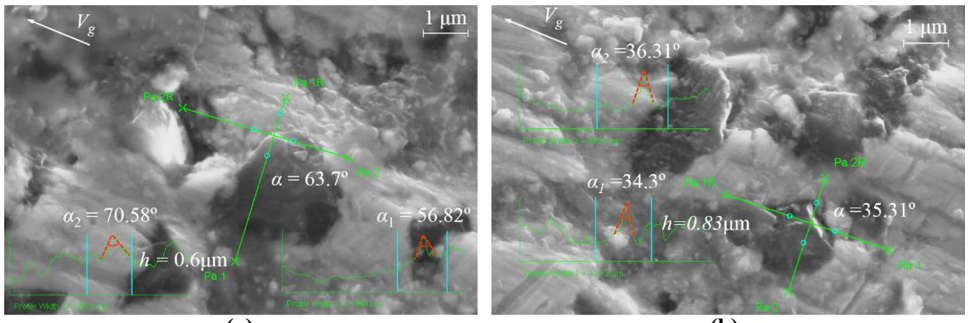

Fig. 11 SEM images of diamond grains after 1.5 min of truing/dressing with and without ultrasonic vibrations. **a** Without ultrasonic vibrations, **b** with ultrasonic vibrations at $A_{p\text{-}p} = 4.7$ μm

before truing/dressing, but significant differences appeared after truing/dressing with (Fig. 8b') and without (Fig. 8b) ultrasonic vibrations for 1.5 min. Compared with the case in the absence of ultrasonic vibrations, the falling off of abrasive grains and the shedding of resin bond material were significantly reduced in the presence of ultrasonic vibrations, which was likely due to the significant decrease in the truing/dressing force caused by the ultrasonic vibrations.

In the same statistical area, the number of effective grains and the total number of grains in the region were counted, and the percentage of the effective abrasive grains was calculated. The number of abrasive grains in each area was between 80 and 120. The obtained results demonstrated that the percentage of effective grains was about 5% before truing/dressing, as shown in Fig. 8a and a', which was because a large number of abrasive grains were buried by the bond material. The effect of the ultrasonic vibrations on the percentage of effective grains after 1.5 min of truing/dressing is shown in Fig. 9. This figure illustrates that the percentage of the effective grains increased from 9.2% to 14% as the amplitude increased from $A_{p\text{-}p} = 0$ to 3.6 μm. This phenomenon might be attributed to the increase in the cutting speed of the GC grains relative to the grinding wheel bond material and the extremely increased acceleration of the grinding wheel, which in turn caused the wheel bond material to withstand an impact force owing to the ultrasonic vibrations. Eventually, the combination of these two effects resulted in an increase in the number of effective grains. However, when the ultrasonic amplitude continued to increase, the percentage of effective grains shifted to decrease to 11.5% at $A_{p\text{-}p} = 4.7$ μm. This was because a larger amplitude caused an excessive impact force, so that the abrasive grains easily fell off, and the resin bond material easily broke and fell off. This was consistent with the topographies of the grinding wheels after truing/dressing under different ultrasonic amplitudes, as shown in Fig. 10.

To explore the effect of the ultrasonic amplitude on the micro-morphology of the abrasive grains, SEM observations were conducted on the cutting edges of the diamond grains after truing/dressing with and without ultrasonic vibrations. Figure 11a and b shows the typical SEM images of the diamond grains obtained after 1.5 min of truing/dressing with and without ultrasonic vibrations, respectively. In general, the shape of an abrasive grain can be simplified into a cone with a cutting-edge apex angle of α, as illustrated in Fig. 12, and a smaller value of α corresponds to a sharper grain cutting edge. Therefore, as shown in Fig. 11, the grain cutting-edge apex angle α_1 in the direction of the grain cutting velocity V_g (or V_f) and α_2 in the direction perpendicular to the cutting velocity V_g were measured by SEM, and the average value of $\alpha = (\alpha_1 + \alpha_2)/2$ was regarded as the cutting-edge apex angle of the current grain.

Subsequently, either on the working surface of the grinding wheel after truing/dressing with ($A_{p\text{-}p} = 4.7$ μm) or without ultrasonic vibrations, ten abrasive grains were randomly selected, and their α values were obtained, as shown in Table 2. The result demonstrated that the average cutting-edge apex angle of 10 abrasive grains without ultrasonic vibrations was 52.46°, whereas that with ultrasonic vibrations was 41.05°, indicating the sharper grains were achieved after truing/dressing with ultrasonic vibrations than without.

3.4 Truing/dressing ratio

The cup-shaped GC wheel will become worn during truing/dressing. To characterize the wear rate of the GC wheel, the truing/dressing ratio ξ was obtained using Eq. (4). Figure 13 shows the effect of the ultrasonic amplitude $A_{p\text{-}p}$ on the truing/dressing ratio ξ. Evidently, the value of ξ tended to increase

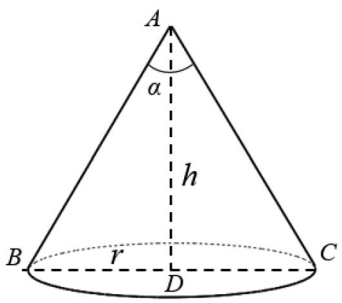

Fig. 12 Simplified conical mode for diamond grains

Table 2 Cutting-edge angles of diamond grains after truing/dressing with and without ultrasonic vibrations

Grain No	α without ultrasonic	Grain No	α with ultrasonic
1	20.2	11	18.4
2	40	12	32.5
3	43	13	34.3
4	51.2	14	36.3
5	57.4	15	38.1
6	57.5	16	40.5
7	58.8	17	42.6
8	61	18	54
9	62.9	19	55.8
10	72.6	20	58
Average value	52.46		41.05

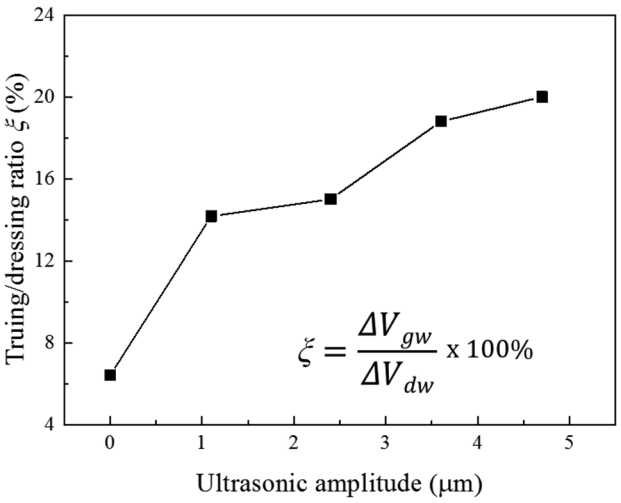

Fig. 13 Effect of ultrasonic amplitude on the truing/dressing ratio ξ

with the increase in $A_{p\text{-}p}$, showing that the truing/dressing ratio dramatically increased from 6.4% to 20% in the range of $A_{p\text{-}p}$ = 0–4.7 μm. This implied that the introduction of ultrasonic vibrations can considerably improve the working lives of GC wheels.

4 Grinding performance test

To evaluate the effectiveness of the proposed truing/dressing method, grinding tests were conducted involving zirconia ceramic workpieces to compare the performances of the diamond grinding wheels trued/dressed with and without ultrasonic vibrations in terms of the work surface roughness and grinding force. In the tests, the grinding wheel rotation speed, the workpiece feed rate, and the wheel depth of cut were set to 4000 r/min, 40 mm/min, and 2 μm, respectively. In addition, the ultrasonic vibration of $A_{p\text{-}p}$ = 4.7 μm was also applied to the grinding wheel during grinding.

After grinding, the morphologies and roughness values of the work surfaces obtained with the grinding wheels trued/dressed with and without ultrasonic vibrations were characterized using a light interferometer (Taylor Hobson CCI HD), as shown in Fig. 14. The surface roughness obtained is perpendicular to the wheel feed rate. A comparison of Fig. 14a with b reveals that the work surface roughness R_a obtained with the grinding wheel trued/dressed with ultrasonic vibrations was 22.26 nm, which was around 25% smaller than the R_a obtained with the grinding wheel trued/dressed without ultrasonic vibrations of 29.58 nm. This may have been because the distribution density of the effective abrasive grains on the work surface of the grinding wheel trued/dressed with ultrasonic vibrations was higher than that without (as analyzed in Sect. 3.3), leading to the improvement of the work surface finish.

Meanwhile, the normal grinding force F_x during grinding was also obtained, as shown in Fig. 15. Compared with the value of F_x obtained with the grinding wheel trued/dressed without ultrasonic vibrations, the value of F_x obtained with the grinding wheel trued/dressed with ultrasonic vibrations was significantly smaller. This was likely because the

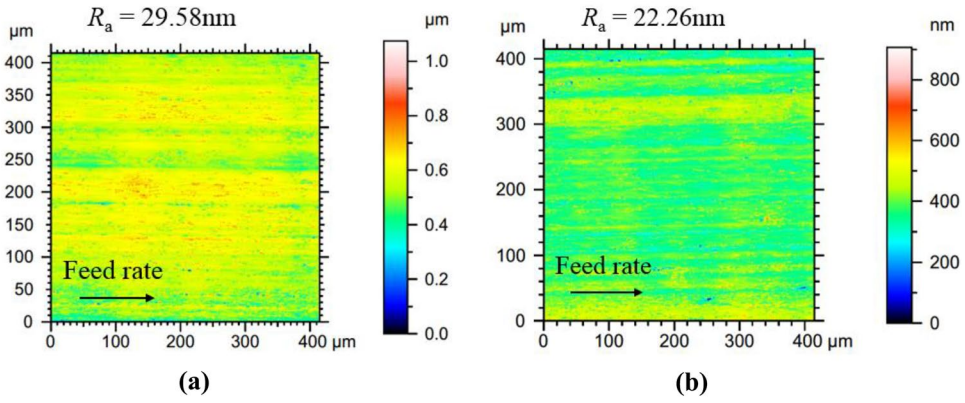

Fig. 14 Morphologies and roughness values of work surfaces obtained by ultrasonic-assisted grinding using grinding wheel with and without ultrasonic vibrations. **a** With grinding wheel trued/dressed for 1.5 min without ultrasonic vibrations, **b** with grinding wheel trued/dressed for 1.5 min with ultrasonic vibration

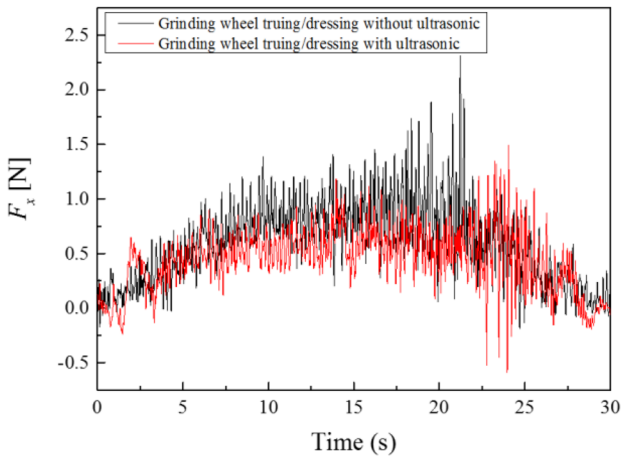

Fig. 15 Grinding force F_x using grinding wheel trued/dressed with and without ultrasonic vibrations

abrasive grain cutting-edge sharpness trued/dressed with ultrasonic vibrations was higher than that without ultrasonic vibrations, as mentioned in Sect. 3.3.

5 Conclusion

An ultrasonic-assisted truing/dressing method using a cup-shaped GC wheel was proposed for truing/dressing metal–resin-bonded diamond grinding wheels. An experimental apparatus for performing the proposed method was constructed, and a series of experiments were conducted to characterize its performance. The obtained results are summarized as follows:

(1) The truing/dressing force F_x decreased and tended to be stable during truing/dressing, and as the ultrasonic amplitude increased, F_x also decreased.

(2) The shape accuracy, i.e., the radial runout and the axial straightness, of the grinding wheel were significantly improved with the assistance of ultrasonic vibrations during truing/dressing. In addition, the improvement rate of the wheel shape accuracy increased with the increase in the ultrasonic amplitude, showing that a higher ultrasonic amplitude resulted in a higher truing/dressing efficiency.

(3) In the range of ultrasonic amplitudes of $A_{p\text{-}p}$ = 0–4.7 μm, the highest distribution density of the effective abrasive grains on the grinding wheel working surface was attained at $A_{p\text{-}p}$ = 3.6 μm. Moreover, during truing/dressing, the introduction of ultrasonic vibrations reduced the abrasive grain cutting-edge apex angle, meaning the sharpness of the grain cutting edge was improved by the ultrasonic treatment.

(4) The truing/dressing ratio increased with the increase in the ultrasonic amplitude, leading to the extension of the working life of the cup-shaped GC wheel.

Finally, comparing the performances of the grinding wheels trued/dressed with and without ultrasonic vibrations in the grinding of zirconia ceramics revealed that the grinding wheel trued/dressed with ultrasonic vibrations yielded better work surfaces and lower grinding forces.

Acknowledgements This work was financially supported by the Key projects of the Ministry of Science and Technology of China (Grant No. 2021YFF0700900), the National Nature Science Foundation of China (Grant No.51975269), and the Shenzhen Science and Technology Program (Grant No. KQTD20170810110250357)

Authors contributions The corresponding author Yongbo Wu has guided the paper writing and contributed to data discussion and article revision. Jiaping Qiao was responsible for writing, developing the experimental designs and measurements, and analyzing experimental results. Hanqiang Wu and Linhe Sun were responsible for assisting in experiments and improving the test jigs. Ming Feng assisted in data processing and paper revision. Jiang Zeng took part in ensuring experimental environment and preparing workpieces.

Funding Funding for this study was obtained from the Key projects of the Ministry of Science and Technology of China (Grant No. 2021YFF0700903), the National Nature Science Foundation of China (Grant No.51975269), and the Shenzhen Science and Technology Program (Grant No. KQTD20170810110250357).

Availability of data and materials The authors confirm that all data generated or analyzed and materials during this study are included in this article.

Declarations

Ethical Approval Not applicable.

Consent to Participate Not applicable.

Consent to Publish Not applicable.

Competing Interests The authors declare that they have no conflict of interest.

References

1. Chen FJ, Yin SH, Huang H, Ohmori H, Zhu YJ (2010) Profile error compensation in ultra-precision grinding of aspheric surfaces with on-machine measurement. Int J Mach Tools Manuf 50(5):480–486. https://doi.org/10.1016/j.ijmachtools.2010.01.001
2. Chen B, Guo B, Zhao Q, Wang J, Ge C (2016) On-machine precision form truing of resin bonded arc-shaped diamond wheels. J Mech Eng 52(11):193–200

3. Qiao J, Feng M, Li Y, Li S, & Wu Y (2021) A study on tangential ultrasonic-assisted mirror grinding of zirconia ceramic curved surfaces. Int J Adv Manuf Technol 112(9). https://doi.org/10.1007/s00170-020-06512-2
4. Marinescu ID (2007) Handbook of Advanced Ceramics Machining. CRC Press
5. Liu YF, Jing JT, Li ZJ (2012) Relationship between bond patterns of tools and working performance in rotary ultrasonic grinding. Opt Precis Eng 20(9):2021–2028
6. Brinksmeier E, Mutlugünes Y, Klocke F, Aurich JC, Shore P, Ohmori H (2010) Ultra-precision grinding. CIRP Ann Manuf Technol 59(2):652–671. https://doi.org/10.1016/j.cirp.2010.05.001
7. Lin XH, Wang ZZ, Guo YB, Peng YF, Hu CL (2014) Research on the error analysis and compensation for the precision grinding of large aspheric mirror surface. Int J Adv Manuf Technol 71(1–4):233–239. https://doi.org/10.1007/s00170-013-5430-y
8. Guo YB, Yang W, Wang ZZ (2013) Technology and application of ultra-precision machining for large size optic. J Mech Eng 49(19):171–178. https://doi.org/10.3901/JME.2013.19.171
9. Zhao QL, Guo B (2012) Ultraprecision grinding technology of microstructured optical functional molds. J Mech Eng 47(21):177–185. https://doi.org/10.3901/JME.2011.21.177
10. Chen M, LI Z, Bo Y U, Peng H, & Fang Z. (2013) On-machine precision preparation and dressing of ball-headed diamond wheel for the grinding of fused silica. J Mech Eng 26(005):982–987. https://doi.org/10.3901/CJME.2013.05.982
11. Rahman MS, Saleh T, Lim HS, Son SM (2008) Development of an on-machine profile measurement system in ELID grinding for machining aspheric surface with software compensation. Int J Mach Tools Manuf 48(7–8):887–895. https://doi.org/10.1016/j.ijmachtools.2007.11.005
12. Xie J, Zhou RM, Xu J, Zhong YG (2010) Form-truing error compensation of diamond grinding wheel in CNC envelope grinding of free-form surface. Int J Adv Manuf Technol 48(9–12):905–912. https://doi.org/10.1007/s00170-009-2338-7
13. Stompe M, Witzendorff P V, Cvetkovic S, Moalem A, Stute U, & Rissing L (2012) Concept for performance-enhancement of ultra-precision dicing for bulk hard and brittle materials in micro applications by laser dressing. Microelectron Eng 98(OCT.): 544–547. https://doi.org/10.1016/j.mee.2012.07.033
14. Huang H (2001) Effects of truing/dressing intensity on truing/dressing efficiency and grinding performance of vitrified diamond wheels. J Mater Process Technol 117(1):9–14. https://doi.org/10.1016/S0924-0136(01)01004-4
15. Takagi J, Liu M (1996) Fracture characteristics of grain cutting edges of CBN wheel in truing operation. J Mater Process Technol 62(4):397–402. https://doi.org/10.1016/S0924-0136(96)02442-9
16. Sanchez JA, Pombo I, Cabanes I, Ortiz R, Lacalle L (2008) Electrical discharge truing of metal-bonded CBN wheels using single-point electrode. Int J Mach Tools Manuf 48(3–4):362–370. https://doi.org/10.1016/j.ijmachtools.2007.10.002
17. Cai LR, Jia Y, Hu DJ (2009) Dressing of metal-bonded super abrasive grinding wheels by means of mist-jetting electrical discharge technology. J Mater Process Technol 209(2):779–784. https://doi.org/10.1016/j.jmatprotec.2008.02.052
18. Ohmori H, Nakagawa T (1995) Analysis of mirror surface generation of hard and brittle materials by ELID (electronic in-process dressing) grinding with superfine grain metallic bond wheels. CIRP Ann 44(1):287–290. https://doi.org/10.1016/S0007-8506(07)62327-0
19. Itoh N, Ohmori H (2004) Development of metal-free conductive bonded diamond wheel for environmentally-friendly electrolytic in-process dressing (ELID) grinding. New Diamond & Frontier Carbon Technology An Int J New Diamond Front Carbon & Related Mater 14(4):227–238
20. Nomura M, Wu Y, Kato M, Kuriyagawa T (2005) Effects of ultrasonic vibration in truing and dressing of CBN grinding wheel used for internal grinding of small holes. Key Eng Mater 291–292:183–188. https://doi.org/10.4028/www.scientific.net/KEM.291-292.183
21. Beaucamp A, Katsuura T, Takata K (2018) Process mechanism in ultrasonic cavitation assisted fluid jet polishing. Cirp Annals, S0007850618300994. https://doi.org/10.1016/j.cirp.2018.04.075
22. Setti D, Ghosh S, Rao PV (2017) A method for prediction of active grits count in surface grinding. Wear 382–383:71–77. https://doi.org/10.1016/j.wear.2017.04.012
23. Jamshidi H, Gurtan M, Budak E (2019) Identification of active number of grits and its effects on mechanics and dynamics of abrasive processes. J Mater Process Technol. https://doi.org/10.1016/j.jmatprotec.2019.05.020